On a simplified mechanical energy budget of Titan's subsurface ocean: a fluid-structure interaction problem[1]

Eric Deleersnijder and David Vincent, 8 July 2020

Abstract. The top boundary of the water-filled global ocean of Titan, Saturn's biggest moon, is an ice layer that is modelled herein as a visco-elastic material. The energy budget of inviscid flows taking place in the ocean is established, taking into account the potential energy associated with the top ice layer as well as the energy dissipated in it. Four types of flow models are examined, ranging from a three-dimensional, non-hydrostatic baroclinic representation, i.e. the most complex one, to the simplest one, which is represented by depth-integrated equations. For all the models, the time rate of change of the mechanical energy (the sum of the kinetic energy and the various types of potential energies) is due to the power dissipated in the top ice layer (i.e. in its “damping” component). The formulation of the kinetic and the potential energies depend on the flow model under consideration.

Introduction

As several other icy moons of the Solar System, Titan (the largest moon of Saturn) houses a global subsurface ocean filled with liquid water and ammonia/salts beneath its icy surface. The presence of such an ocean was first predicted in [1], although it had already been evoked in [2]. Several observations and measurements such as Titan’s obliquity, the gravitational tides and electric signals support this assumption [3, 4, 5, 6, 7, 8, 9, 10]. While the presence of an ocean is widely acknowledged, some of its characteristics are poorly constrained. Several models were developed to derive Titan’s internal structure and, hence, the characteristics of the layers. Most of them agree that four main layers can be identified (Figure 1): the core (made of silicates or a rock-iron mixture, depending on the model under consideration), a high-pressure (water) ice layer, a liquid layer, and the surface ice layer.

The global, subsurface liquid layer modifies the magnetic field, ability to deform, and shape of the moon. The liquid motion in such an ocean is driven by the tidal forcing, the temperature gradient resulting from the bottom and surface heat fluxes, and the deformation of the adjacent layers. The vertical uplifting of the high pressure ice layer at the bottom of the ocean reduces the actual tidal forcing acting on the ocean. This can be modelled by an attenuation factor, which is a function of the second degree tidal and radial Love numbers. The deformation of the upper ice layer results in a surface pressure acting on the ocean. This pressure can be related to the ocean surface elevation and/or the time derivative of the ocean surface elevation, depending on the mechanical behaviour of the ice shell [11].

The ice shell therefore impacts the energy balance of the ocean. It modifies the amount of kinetic energy dissipated by friction as an upper viscous boundary layer develops and results in dissipation of potential energy due to the interactions between the ocean and ice shell [12].

[1] This working note is a tentative answer to a question asked by Prof Vincent Legat during David Vincent's private PhD thesis defence.

We will study the energy budget of the ocean under different assumptions as to the mechanical properties of the fluid flow taking place in the subsurface ocean. The latter is dealt with on the f-plane for the sake of simplicity and because we believe this representation encompasses the processes that are crucial for the mechanical energy budget of the ocean.

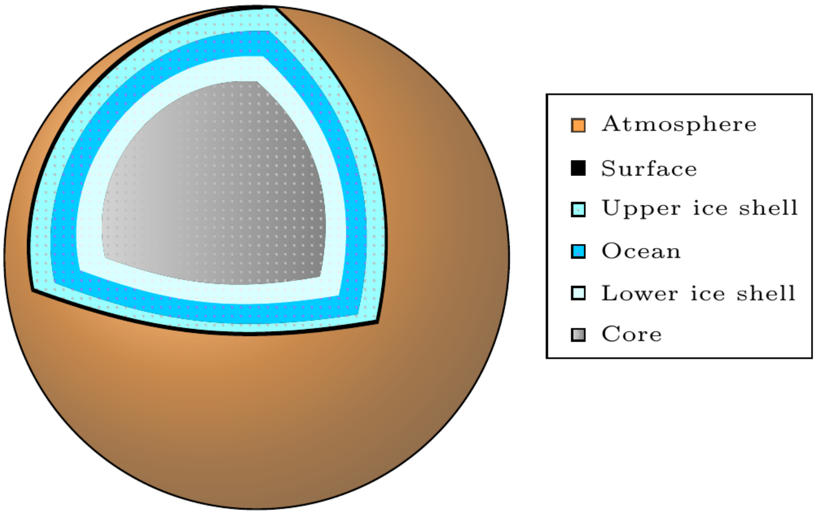

Figure 1. Internal structure of Titan as is presently conceived by the scientific community. The thickness of each layer is not to scale for the sake of clarity. The schematic is taken from [11].

Boundaries of the domain of interest

Let x and y represent horizontal coordinates, whilst z is the vertical one, increasing upward. Accordingly, the domain of interest is defined as follows:

$$\mathbf{x}_h = (x,y) \in \mathcal{S} \quad , \qquad z \in \left[-h(\mathbf{x}_h), \eta(t,\mathbf{x}_h)\right] \quad , \tag{1}$$

where $\mathcal{S} \subset \Re^2$; t is the time; $h(\mathbf{x}_h)$ and $\eta(t,\mathbf{x}_h)$ is the unperturbed ocean depth and the ocean surface elevation, respectively (Figure 2).

Let $\mathbf{e}_z$ be a unit vector pointing upward. Then, $\mathbf{x} = \mathbf{x}_h + z\mathbf{e}_z$ is the position vector. The velocity field is denoted

$$\mathbf{v}(t,\mathbf{x}) \;=\; \mathbf{u}(t,\mathbf{x}) \;+\; w(t,\mathbf{x})\,\mathbf{e}_z \quad , \tag{2}$$

where $\mathbf{u}$ is the horizontal velocity and w is the vertical component of the velocity. On the "lateral boundary" (i.e. the boundary of $\mathcal{S}$), periodicity boundary conditions are prescribed, for the ocean is global. The upper and lower boundaries, Γ^s and Γ^b, with $\Gamma = \Gamma^s \cup \Gamma^b$, are impermeable, leading us to prescribe boundary condition

$$\left[(\mathbf{v} - \mathbf{v}^{\Gamma}) \bullet \mathbf{n}\right]_{\mathbf{x}\in\Gamma} \;=\; 0 \quad , \tag{3}$$

where $\mathbf{n}$ is the outward unit normal to Γ and $\mathbf{v}^{\Gamma}$ is the velocity of the boundary. As the lower boundary is assumed to be motionless, $\mathbf{v}^{\Gamma}$ is zero at $z = -h(x,y)$, yielding impermeability condition

$$\left[\mathbf{u}\bullet\nabla_h h + w\right]_{z=-h} = 0 \quad . \tag{4}$$

The upper boundary is the interface between the oceanic fluid and the ice layer lying on top of it. Its velocity may be taken to be [13]

$$\mathbf{v}^{\Gamma} = \frac{\partial\eta}{\partial t}\mathbf{e}_z \quad . \tag{5}$$

The associated impermeability condition reads

$$\left[\frac{\partial\eta}{\partial t} + \mathbf{u}\bullet\nabla_h\eta - w\right]_{z=\eta} = 0 \tag{6}$$

Clearly, (4) and (6) are derived from general impermeability condition (3).

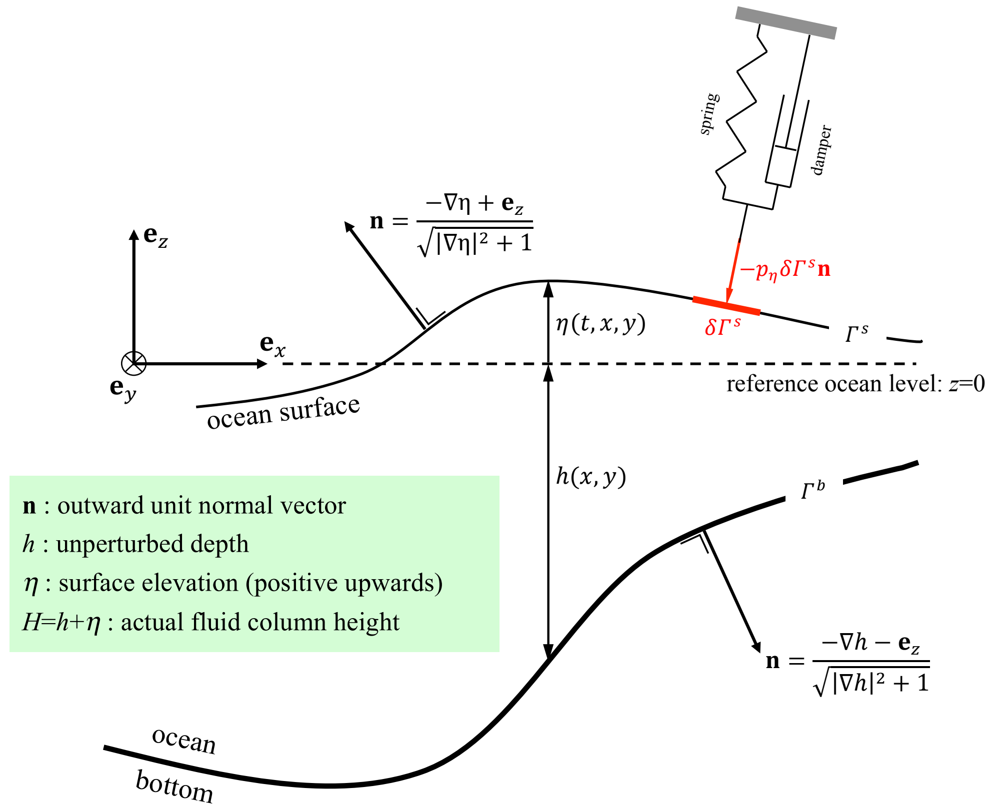

Figure 2. Illustration of the geometry of the global ocean (in the horizontal-vertical plane) and the ice layer lying on top of the fluid column, which is modelled as a massless spring-damper system (visco-elastic behaviour).

The ice layer is assumed to be a massless visco-elastic material, which is represented schematically by a spring and a damper connected in parallel (Figure 2). Accordingly, the pressure at the upper boundary, $p_\eta = [p]_{z=\eta}$, tends to nudge the interface towards its unperturbed position ($z=0$):

$$p_\eta = p_{\bullet} + A\eta + B\frac{\partial\eta}{\partial t} \quad , \tag{7}$$

where constant $p_\bullet$ is an appropriate reference pressure (whose value is unimportant in the present study); A ($\mathrm{N\,m^{-1}/m^2}$) is the spring constant (measuring its stiffness) per unit surface and B ($\mathrm{N\,s\,m^{-1}/m^2}$) is the damping coefficient per unit surface. For the sake of simplicity, A and B are assumed to be constant (Table 1).

Table 1. Exact or plausible values of the parameters of the models tackled herein. It must be stressed that parameters A and B are not independent of each other [11].

parameter	value	units
radius: R	2.574×10^{6}	m
angular velocity: $\lvert\boldsymbol{\omega}\rvert$	4.56×10^{-6}	s
gravitational acceleration: g	1.352	$\mathrm{m\,s^{-2}}$
ocean depth: h	$10^{5}-4\times10^{5}$	m
reference density: $\rho_\bullet$	$1.10\times10^{3}-1.35\times10^{3}$	$\mathrm{kg\,m^{-3}}$
spring stiffness (per unit surface): A	$\begin{cases}\text{elastic ice: } 80\\ \text{viscoelastic ice: } 60\\ \text{liquid ice: } 35\end{cases}$	$\mathrm{N\,m^{-1}/m^2}$
damping coefficient (per unit surface): B	$\begin{cases}\text{elastic ice: } 4.0\\ \text{viscoelastic ice: } 23\\ \text{liquid ice: } 5.7\end{cases}$	$\mathrm{N\,s\,m^{-1}/m^2}$

Inviscid flow model

The Boussinesq approximation is assumed to hold valid in the global ocean (which is the reason why the value of reference pressure $p_\bullet$ is unimportant). The (constant) reference density is denoted $\rho_\bullet$, whilst the actual value of the fluid density is $\rho(t,\mathbf{x})$. Then, the continuity equation reads

$$\nabla\bullet\mathbf{v} = 0 \quad , \tag{8}$$

where ∇ represents the del operator.

All diffusive processes are assumed to be negligible. Accordingly, the momentum equation is

$$\rho_\bullet D_t\mathbf{v} + \rho_\bullet\boldsymbol{\omega}\times\mathbf{v} = -\nabla p - \rho g\mathbf{e}_z \quad , \tag{9}$$

where $\boldsymbol{\omega}$ is Titan's angular velocity vector and constant g is the gravitational acceleration; D_t denotes the material derivative, i.e.

$$D_t = \frac{\partial}{\partial t} + \mathbf{v}\bullet\nabla = \frac{\partial}{\partial t} + \mathbf{u}\bullet\nabla_h + w\frac{\partial}{\partial z} \quad , \tag{10}$$

where $\nabla_h = \nabla - \mathbf{e}_z\,\partial/\partial z$ is the horizontal part of the del operator. Under the abovementioned assumptions and in the absence of any heat source, the entropy equation simplifies to [14]

$$D_t\,\rho = 0 \quad . \tag{11}$$

This equation is to be solved under periodicity boundary conditions on the lateral boundaries and

$$\left[\rho(\mathbf{v}-\mathbf{v}^{\Gamma})\bullet\mathbf{n}\right]_{\mathbf{x}\in\Gamma} = 0 \tag{12}$$

on the upper and lower boundaries of the domain.

Reynolds' transport theorem for a material volume

Hereinafter, we will deal with various integrals over the domain or its boundary. In view of the boundary conditions applied to the velocity field, the domain of interest, Ω, actually is a material volume, allowing us to use a special version of Reynold's transport theorem.

According to the aforementioned theorem, any function of time and position, $\xi(t,\mathbf{x})$, satisfies

$$\frac{d}{dt}\int_{\Omega}\xi\,d\Omega = \int_{\Omega}\frac{\partial\xi}{\partial t}\,d\Omega + \int_{\Gamma}\xi\,\mathbf{v}^{\Gamma}\bullet\mathbf{n}\,d\Gamma \quad . \tag{13}$$

Using (3), (8) and the divergence theorem allows transforming the last term of (13) as follows:

$$\int_{\Gamma}\xi\,\mathbf{v}^{\Gamma}\bullet\mathbf{n}\,d\Gamma = \int_{\Gamma}\xi\,\mathbf{v}\bullet\mathbf{n}\,d\Gamma = \int_{\Omega}\nabla\bullet(\xi\,\mathbf{v})\,d\Omega = \int_{\Omega}\mathbf{v}\bullet\nabla\xi\,d\Omega \quad . \tag{14}$$

Then, substituting (14) into (13) and having recourse to definition (10) of the material derivative, we obtain a well-known integral relation

$$\frac{d}{dt}\int_{\Omega}\xi(t,\mathbf{x})\,d\Omega = \int_{\Omega}D_t\left[\xi(t,\mathbf{x})\right]d\Omega \quad . \tag{15}$$

This relation may be first resorted to in order to prove that volume V of the fluid under study and its mass M are time-independent (as they should be):

$$\frac{dV}{dt} = \frac{d}{dt}\underbrace{\int_{\Omega}1\,d\Omega}_{=V} = \underbrace{\int_{\Omega}D_t 1\,d\Omega}_{\substack{=0\,,\\ \text{since } D_t 1=0}} = 0 \quad\Rightarrow\quad V = const. \tag{16}$$

$$\frac{dM}{dt} = \frac{d}{dt}\underbrace{\int_{\Omega}\rho\,d\Omega}_{=M} = \underbrace{\int_{\Omega}D_t\rho\,d\Omega}_{=0,\ \text{see (11)}} = 0 \quad\Rightarrow\quad M = const. \tag{17}$$

Next, with the help of (15), we will investigate the energetics of the flow under consideration taking into account the impact of the ice layer.

Energetics

To obtain the equation governing the mechanical energy of the flow, momentum equation (9) is multiplied by the velocity and integrated over the domain. Then, appropriate manipulations are carried out with the aim of identifying the relevant energy forms. Accordingly, we will deal below with each term of (9).

The first term in the left-hand side of (9) leads to

$$\int_{\Omega} (\rho_{\bullet} D_t \mathbf{v}) \bullet \mathbf{v} \, d\Omega = \int_{\Omega} D_t \left(\frac{\rho_{\bullet}}{2} |\mathbf{v}|^2 \right) d\Omega = \frac{d}{dt} \underbrace{\int_{\Omega} \frac{\rho_{\bullet}}{2} |\mathbf{v}|^2 \, d\Omega}_{=K} \tag{18}$$

where K denotes the kinetic energy. Then, it is easily seen that the power developed by the Coriolis force is identically zero,

$$\int_{\Omega} (-\rho_{\bullet} \boldsymbol{\omega} \times \mathbf{v}) \bullet \mathbf{v} \, d\Omega = 0 \quad . \tag{19}$$

This is because vector $\boldsymbol{\omega} \times \mathbf{v}$ is always orthogonal to velocity $\mathbf{v}$.

Using (5), the divergence theorem and identity $\mathbf{e}_z \bullet \mathbf{n} \delta\Gamma^s = \delta\mathcal{S}$ (which may be seen to hold valid from a simple inspection of Figure 2), the power developed by the pressure force is

$$\begin{aligned} P_p &= \int_{\Omega} (-\nabla p) \bullet \mathbf{v} \, d\Omega = \int_{\Omega} \nabla \bullet (-p\mathbf{v}) \, d\Omega + \overbrace{\int_{\Omega} p \nabla \bullet \mathbf{v} \, d\Omega}^{=0, \text{ see (8)}} \\ &= \int_{\Gamma^s} -p_\eta \mathbf{v}^\Gamma \bullet \mathbf{n} \, d\Gamma^s = \int_{\Gamma^s} -p_\eta \frac{\partial \eta}{\partial t} \mathbf{e}_z \bullet \mathbf{n} \, d\Gamma^s = \int_{\mathcal{S}} -p_\eta \frac{\partial \eta}{\partial t} \, d\mathcal{S} \end{aligned} \tag{20}$$

Combining (7) and (20) yields

$$\begin{aligned} P_p &= \int_{\mathcal{S}} -p_\eta \frac{\partial \eta}{\partial t} \, d\mathcal{S} = \int_{\mathcal{S}} -\left(p_{\bullet} + A\eta + B\frac{\partial \eta}{\partial t} \right) \frac{\partial \eta}{\partial t} \, d\mathcal{S} \\ &= -p_{\bullet} \underbrace{\int_{\mathcal{S}} \frac{\partial \eta}{\partial t} \, d\mathcal{S}}_{\substack{=0, \text{ since} \\ V = const.}} - \frac{d}{dt} \underbrace{\int_{\mathcal{S}} \frac{A}{2} \eta^2 \, d\mathcal{S}}_{U_s} + \underbrace{\int_{\mathcal{S}} \left[-B \left(\frac{\partial \eta}{\partial t} \right)^2 \right] d\mathcal{S}}_{=P_d} \end{aligned} \tag{21}$$

where U_s is the potential energy related to the "spring" (i.e. the elastic part of the behaviour of the upper ice layer), whilst negative definite term P_d is the power dissipated by the "damper" (i.e. the viscous part of the behaviour of the upper ice layer).

The power developed by the weight of the fluid reads

$$\begin{aligned} P_g &= \int_{\Omega} (-\rho g \mathbf{e}_z) \bullet \mathbf{v} \, d\Omega = \int_{\Omega} (-\rho g w) \, d\Omega = \int_{\Omega} [-\rho g D_t (z - z_{\bullet})] \, d\Omega \\ &= \int_{\Omega} D_t [-\rho g (z - z_{\bullet})] \, d\Omega + \underbrace{\int_{\Omega} (D_t \rho) g (z - z_{\bullet}) \, d\Omega}_{=0, \text{ see (11)}} = -\frac{d}{dt} \underbrace{\int_{\Omega} \rho g (z - z_{\bullet}) \, d\Omega}_{U_g} \end{aligned} \tag{22}$$

where $z_{\bullet}$ is an appropriate reference level and U_g denotes the gravitational potential energy.

The latter may be split into three contributions as follows

$$U_g = \underbrace{\int_{\Omega} (\rho-\rho_{\bullet})g(z-z_{\bullet})\,d\Omega}_{=U_g^{bc}} + \underbrace{\int_{\mathcal{S}} \frac{\rho_{\bullet}g}{2}\eta^2\,d\mathcal{S}}_{=U_g^{bt}} + \underbrace{\int_{\mathcal{S}} \frac{\rho_{\bullet}g}{2}h^2\,d\mathcal{S} - \rho_{\bullet}gz_{\bullet}V}_{=const.} \qquad (23)$$

where U_g^{bc} (resp. U_g^{bt}) is the baroclinic (resp. barotropic) available gravitational potential energy. The last term of (23) is constant. Therefore, it plays no role in the energy budget and, hence, will be ignored below.

Table 2. Governing equations, kinetic (K) and potential (U_g^{bc}, U_g^{bt}, U_s) energies, and (negative definite) power (P_d) developed by the only non-conservative force in four classical types of inviscid geophysical flow models that could possibly be applied to Titan's global, subsurface ocean.

model type	governing equations	energetics
3D, non-hydrostatic, baroclinic	$\nabla \bullet \mathbf{v} = 0$ $\rho_{\bullet} D_t\mathbf{v} + \rho_{\bullet}\boldsymbol{\omega}\times\mathbf{v} = -\nabla p - \rho g \mathbf{e}_z$ $D_t\rho = 0$	$K = \int_{\Omega} \frac{\rho_{\bullet}}{2}\lvert\mathbf{v}\rvert^2\,d\Omega$ $U_g^{bc} = \int_{\Omega}(\rho-\rho_{\bullet})g(z-z_{\bullet})\,d\Omega$, $U_g^{bt} = \int_{\mathcal{S}}\frac{\rho_{\bullet}g}{2}\eta^2\,d\mathcal{S}$ $U_s = \int_{\mathcal{S}}\frac{A}{2}\eta^2\,d\mathcal{S}$, $P_d = \int_{\mathcal{S}}\left[-B\left(\frac{\partial\eta}{\partial t}\right)^2\right]d\mathcal{S}$
3D, hydrostatic, baroclinic	$\nabla \bullet \mathbf{v} = 0$ $\rho_{\bullet} D_t\mathbf{u} + \rho_{\bullet} f\mathbf{e}_z\times\mathbf{u} = -\nabla_h p$ $0 = -\frac{\partial p}{\partial z} - \rho g$ $D_t\rho = 0$	$K = \int_{\Omega} \frac{\rho_{\bullet}}{2}\lvert\mathbf{u}\rvert^2\,d\Omega$ $U_g^{bc} = \int_{\Omega}(\rho-\rho_{\bullet})g(z-z_{\bullet})\,d\Omega$, $U_g^{bt} = \int_{\mathcal{S}}\frac{\rho_{\bullet}g}{2}\eta^2\,d\mathcal{S}$ $U_s = \int_{\mathcal{S}}\frac{A}{2}\eta^2\,d\mathcal{S}$, $P_d = \int_{\mathcal{S}}\left[-B\left(\frac{\partial\eta}{\partial t}\right)^2\right]d\mathcal{S}$
3D, hydrostatic, barotropic	$\nabla \bullet \mathbf{v} = 0$ $\rho_{\bullet} D_t\mathbf{u} + \rho_{\bullet} f\mathbf{e}_z\times\mathbf{u} = -\nabla_h p$ $0 = -\frac{\partial p}{\partial z} - \rho_{\bullet} g$ $\rho = \rho_{\bullet}$	$K = \int_{\Omega} \frac{\rho_{\bullet}}{2}\lvert\mathbf{u}\rvert^2\,d\Omega$ $U_g^{bc} = 0$, $U_g^{bt} = \int_{\mathcal{S}}\frac{\rho_{\bullet}g}{2}\eta^2\,d\mathcal{S}$ $U_s = \int_{\mathcal{S}}\frac{A}{2}\eta^2\,d\mathcal{S}$, $P_d = \int_{\mathcal{S}}\left[-B\left(\frac{\partial\eta}{\partial t}\right)^2\right]d\mathcal{S}$
2D, depth-integrated	$\frac{\partial\eta}{\partial t} + \nabla_h \bullet (H\bar{\mathbf{u}}) = 0$ $\rho_{\bullet} D_{h,t}\bar{\mathbf{u}} + \rho_{\bullet} f\mathbf{e}_z\times\bar{\mathbf{u}}$ $= -\rho_{\bullet} g\nabla_h\eta - A\nabla_h\eta - B\nabla_h\left(\frac{\partial\eta}{\partial t}\right)$	$K = \int_{\mathcal{S}} \frac{\rho_{\bullet}H}{2}\lvert\bar{\mathbf{u}}\rvert^2\,d\mathcal{S}$ $U_g^{bc} = 0$, $U_g^{bt} = \int_{\mathcal{S}}\frac{\rho_{\bullet}g}{2}\eta^2\,d\mathcal{S}$ $U_s = \int_{\mathcal{S}}\frac{A}{2}\eta^2\,d\mathcal{S}$, $P_d = \int_{\mathcal{S}}\left[-B\left(\frac{\partial\eta}{\partial t}\right)^2\right]d\mathcal{S}$

The mechanical energy is defined as the sum of the kinetic energy and the potential energies, i.e.

$$E = K + U_g^{bc} + U_g^{bt} + U_s \quad . \tag{24}$$

Then, combining all of the results obtained above yields

$$\frac{dE}{dt} = \frac{d}{dt}\underbrace{\left(K + U_g^{bc} + U_g^{bt} + U_s\right)}_{=E} = P_d \leq 0 \tag{25}$$

This is a well-known property in the field of mechanics: the time rate of change of the mechanical energy is equal to the power developed by the non-conservative forces. In this case, there is only one such force, i.e. the force associated with the damper, which always dissipates energy. Accordingly, the mechanical energy of the flow under consideration cannot increase.

Most geophysical flow models rely on simplifications that were not taken into account above. This is why it is appropriate to consider simpler models and the related energy forms, which may be somewhat different. The main results thereof are gathered in Table 2.

It must be stressed that the power dissipated in the top ice layer is most likely to be significantly smaller than that dissipated by the ocean bottom and surface shear stresses. They were ignored in this working note, for the formulation and role of such phenomena is well known, which is why they were disregarded in this idealised study focusing on the impact on the energy budget of the top ice layer.

Acknowledgements. Prof. Jean-Marie Beckers offered a useful piece of advice about the concept of available gravitational potential energy.

References

[1] Lunine, J. I., & Stevenson, D. J. (1987). Clathrate and ammonia hydrates at high pressure: Application to the origin of methane on Titan. Icarus, 70(1), 61-77.

[2] Consolmagno, G. J., & Lewis, J. S. (1978). The evolution of icy satellite interiors and surfaces. Icarus, 34(2), 280-293.

[3] Baland, R. M., Van Hoolst, T., Yseboodt, M., & Karatekin, Ö. (2011). Titan's obliquity as evidence of a subsurface ocean?. Astronomy & Astrophysics, 530, A141.

[4] Baland, R. M., Tobie, G., Lefèvre, A., & Van Hoolst, T. (2014). Titan's internal structure inferred from its gravity field, shape, and rotation state. Icarus, 237, 29-41.

[5] Béghin, C., Sotin, C., & Hamelin, M. (2010). Titan's native ocean revealed beneath some 45 km of ice by a Schumann-like resonance. Comptes Rendus Geoscience, 342(6), 425-433.

[6] Hemingway, D., Nimmo, F., Zebker, H., & Iess, L. (2013). A rigid and weathered ice shell on Titan. Nature, 500(7464), 550-552.

[7] Iess, L., Jacobson, R. A., Ducci, M., Stevenson, D. J., Lunine, J. I., Armstrong, J. W., ... & Tortora, P. (2012). The tides of Titan. Science, 337(6093), 457-459.

[8] Lefevre, A., Tobie, G., Choblet, G., & Čadek, O. (2014). Structure and dynamics of Titan's outer icy shell constrained from Cassini data. Icarus, 237, 16-28.

[9] Nimmo, F., & Bills, B. G. (2010). Shell thickness variations and the long-wavelength topography of Titan. Icarus, 208(2), 896-904.

[10] Rappaport, N. J., Iess, L., Wahr, J., Lunine, J. I., Armstrong, J. W., Asmar, S. W., ... & Racioppa, P. (2008). Can Cassini detect a subsurface ocean in Titan from gravity measurements?. Icarus, 194(2), 711-720

[11] Vincent, D. (2020). Titanic results: a numerical study of motion in the liquid bodies of a Saturnian icy moon (doctoral dissertation, Université catholique de Louvain, Louvain-le-Neuve, Belgium)

[12] Tyler, R. H. (2020). Heating of Enceladus due to the dissipation of ocean tides. Icarus, 348.

[13] Deleersnijder E., 2014, Sur la condition d'imperméabilité de la surface de la mer, Note de travail, Université catholique de Louvain, 4 pages, disponible sur la toile à l'adresse suivante: http://hdl.handle.net/2078.1/155238

[14] Kundu P.K. and I.M. Cohen, 2004 (3rd ed.), Fluid Mechanics, Elsevier, 759 pages

----